

Nonlinear Self-Trapping of Matter Waves in Periodic Potentials

Th. Anker¹, M. Albiez¹, R. Gati¹, S. Hunsmann¹, B. Eiermann¹, A. Trombettoni² and M.K. Oberthaler¹

¹ *Kirchhoff Institut für Physik, Universität Heidelberg,
Im Neuenheimer Feld 227, 69120 Heidelberg, Germany*

² *I.N.F.M. and Dipartimento di Fisica, Università di Parma,
parco Area delle Scienze 7A, I-43100 Parma, Italy*

(Dated: February 2, 2008)

We report the first experimental observation of nonlinear self-trapping of Bose-condensed ⁸⁷Rb atoms in a one dimensional waveguide with a superimposed deep periodic potential. The trapping effect is confirmed directly by imaging the atomic spatial distribution. Increasing the nonlinearity we move the system from the diffusive regime, characterized by an expansion of the condensate, to the nonlinearity dominated self-trapping regime, where the initial expansion stops and the width remains finite. The data are in quantitative agreement with the solutions of the corresponding discrete nonlinear equation. Our results reveal that the effect of nonlinear self-trapping is of local nature, and is closely related to the macroscopic self-trapping phenomenon already predicted for double-well systems.

PACS numbers: N03.75.Lm,63.20.Pw

Keywords:

The understanding of coherent transport of waves is essential for many different fields in physics. In contrast to the dynamics of non-interacting waves, which is conceptually simple, the situation can become extremely complex as soon as interaction between the waves is of relevance. Very intriguing and counter intuitive transport phenomena arise in the presence of a periodic potential. This is mainly due to the existence of spatially localized stationary solutions.

In the following we will investigate the dynamics of Bose-condensed ⁸⁷Rb atoms in a deep one dimensional periodic potential, i.e. the matter waves are spatially localized in each potential minimum (tight binding) and are coupled via tunneling to their next neighbors. This system is described as an array of coupled Boson Josephson junctions [1]. The presence of nonlinearity drastically changes the tunneling dynamics [2] leading to new localization phenomena on a macroscopic scale such as discrete solitons, i.e. coherent non-spreading wave packets, and nonlinear self-trapping [3]. These phenomena have also been studied in the field of nonlinear photon optics where a periodic refractive index structure leads to an array of wave guides, which are coupled via evanescent waves [4].

In this letter we report on the first experimental confirmation of the theoretically predicted effect of nonlinear self-trapping of matter waves in a periodic potential [3]. This effect describes the drastic change of the dynamics of an expanding wave packet, when the nonlinearity i.e. repulsive interaction energy, is increased above a critical value. Here the counterintuitive situation arises that although the spreading is expected to become faster due to the higher nonlinear pressure, the wave packet *stops* to expand after a short initial diffusive expansion. Since we observe the dynamics in real space, we can directly measure the wave packet width for different propagation

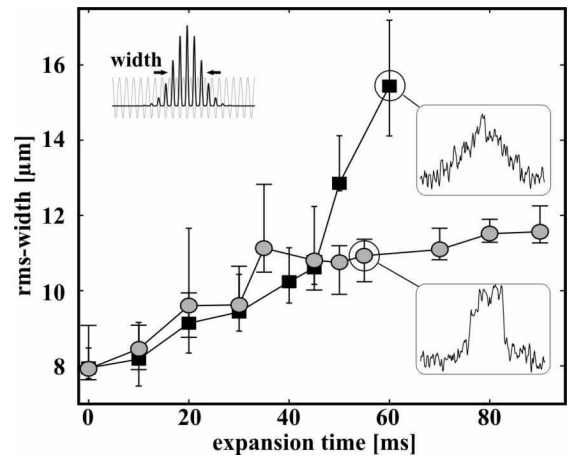


FIG. 1: Observation of nonlinear self-trapping of Bose-condensed ⁸⁷Rb atoms. The dynamics of the wave packet width along the periodic potential is shown for two different initial atom numbers. By increasing the number of atoms from 2000 ± 200 (squares) to 5000 ± 600 (circles), the repulsive atom-atom interaction leads to the stopping of the global expansion of the wave packet. The insets show that the wave packet remains almost gaussian in the diffusive regime but develops steep edges in the self-trapping regime. These edges act as boundaries for the complex dynamics inside.

times. In Fig. 1 we show the experimental signature of the transition from the diffusive to the self-trapping regime. We prepare wave packets in a periodic potential and change only the nonlinear energy by adjusting the number of atoms in the wave packet close to (2000 ± 200) atoms and above (5000 ± 600) atoms the critical value. Clearly both wave packets expand initially. At $t \sim 35$ ms the wave packet with higher initial atomic density has developed steep edges and stops expanding (see inset in Fig. 1). In contrast, the wave packet with the lower initial

atomic density continues to expand keeping its gaussian shape.

The coherent matter-wave packets are generated with ^{87}Rb Bose-Einstein condensates realized in a crossed light beam dipole trap ($\lambda = 1064\text{nm}$, $1/e^2$ waist $55\mu\text{m}$, 600mW per beam). Subsequently a periodic dipole potential $V_p = s \cdot E_r \sin^2(kx)$, realized with a far off-resonant standing light wave ($\lambda = 783\text{nm}$) collinear with one of the dipole trap beams is adiabatically ramped up. The depth of the potential is proportional to the intensity of the light wave and is given in recoil energies $E_r = \frac{\hbar^2 k^2}{2m}$ with the wave vector $k = 2\pi/\lambda$. By switching off the dipole trap beam perpendicular to the periodic potential the atomic matter wave is released into a trap acting as a one-dimensional waveguide $V_{dip} = \frac{m}{2}(\omega_{\perp}^2 r^2 + \omega_{\parallel}^2 x^2)$ with radial trapping frequency $\omega_{\perp} = 2\pi \cdot 230\text{Hz}$ and longitudinal trapping frequency $\omega_{\parallel} \approx 2\pi \cdot 1\text{Hz}$. The wave packet evolution inside the combined potential of the waveguide and the lattice is studied by taking absorption images of the atomic density distribution after a variable time delay. The density profiles $n(x, t)$ along the waveguide are obtained by integrating the absorption images over the radial dimensions and allow the detailed investigation of the wave packet shape dynamics with a spatial resolution of $3\mu\text{m}$.

In Fig. 2 the measured temporal evolution of the wave packet prepared in the self-trapping regime ($s = 10$, $7.6(5)\mu\text{m}$ initial rms-width, 5000 ± 600 atoms) is shown. The evolution of the shape is divided into two characteristic time intervals. Initially ($t < 20\text{ms}$) the wave packet expands and develops steep edges. This dynamics can be understood in a simple way by considering that the repulsive interaction leads to a broadening of the momentum distribution and thus to a spreading in real space. Since the matter waves propagate in a periodic potential the evolution is governed by the modified dispersion (i.e. band structure) $E(q) = -2K \cos(dq)$ where $d = \lambda/2$ is the lattice spacing, $\hbar q$ is the quasimomentum and K is the characteristic energy associated with the tunneling. The formation of steep edges is a consequence of the population of higher quasimomenta around $q = \pm\pi/2d$ where the dispersion is strongly reduced and the group velocity is extremal. In order to populate quasimomenta $|q| > \pi/2d$ the initial interaction energy has to be higher than the characteristic tunneling energy K and thus the critical parameter depends on the ratio between the on-site interaction energy and the tunneling energy as we will discuss in detail. While in the linear evolution the steep edges move with the extremal group velocity [5], in the experiment reported here they stop after their formation. As we will show this is a consequence of the high atomic density gradient at the edge which suppresses tunneling between neighboring wells. The further evolution is characterized by stationary edges acting as boundaries for the complex internal behavior of the wave packet shape. The formation of the side peaks is an indication

that atoms moving outwards are piled up because they cannot pass the steep edge. Finally the pronounced features of the wave packet shape disappear and a square shaped density distribution is formed.

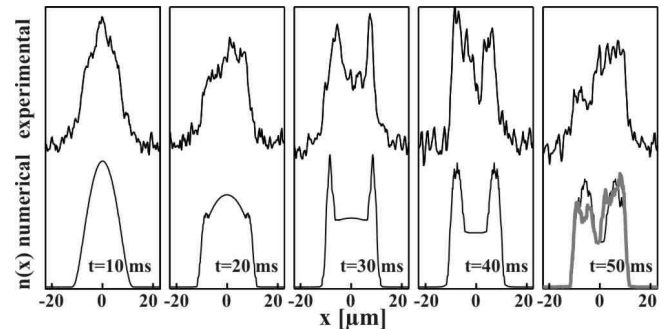


FIG. 2: Comparison between theory and experiment for $s = 10$, $7.6(5)\mu\text{m}$ initial rms-width, and 5000 ± 600 atoms. The upper graphs show the measured density distribution for different propagation times. During the initial expansion in the self-trapping regime the wave packet develops steep edges which act as stationary boundaries for the subsequent internal dynamics. The results of the numerical integration of eq. 2 (depicted in the lower graphs) are in very good agreement. For $t = 50\text{ms}$ a 1.5mrad deviation of the wave guides's horizontal orientation (consistent with the experimental uncertainty) is taken into account and reproduces the experimentally observed asymmetry (gray line).

In order to understand in detail the ongoing complex self-trapping dynamics we compare quantitatively our experimental findings with numerically obtained solutions (see Fig. 2). For our typical experimental parameters of $s \sim 11$ and ~ 100 atoms per well we are in the regime where the dynamics can be described by a macroscopic wave function $\Psi(\vec{r}, t)$ and thus by the Gross-Pitaevski equation (GPE) [6]. Since we use deep optical lattices the description can be reduced to a one dimensional discrete nonlinear equation, which includes the fundamental processes, namely tunneling between the wells and nonlinear phase evolution due to the interaction of the atoms [3, 7]. In our experiment the trapping frequency in a single well along the lattice period is on the order of $\omega_x \approx 2\pi \cdot 25\text{kHz}$, whereas the transverse trapping frequency of the wave guide is $\omega_{\perp} = 2\pi \cdot 230\text{Hz}$. Thus our system can be described as a horizontal pile of pancakes, and the transverse degree of freedom cannot be neglected. In [7] a one dimensional discrete nonlinear equation (DNL) is derived which takes into account the adiabatic change of the wave function in the transverse direction due to the atom-atom interaction. A generalized tight binding ansatz

$$\Psi(\vec{r}, t) = \sum_j \psi_j(t) \Phi_j(\vec{r}, N_j(t)) \quad (1)$$

is used, with $\psi_j(t) = \sqrt{N_j(t)} e^{i\phi_j(t)}$, where $N_j(t)$ is the atom number and $\phi_j(t)$ is the phase of the j th con-

densate. Φ_j is normalized to 1 (i.e. $\int d\vec{r}\Phi_j^2 = 1$) and $\Psi(\vec{r}, t)$ is normalized to the total number of atoms N_T (i.e. $\sum_j |\psi_j|^2 = N_T$). The spatial real wave function $\Phi_j(\vec{r}, N_j(t))$ is centered at the minimum of the j -th well and is time dependent through $N(t)$. Integrating over the spatial degrees of freedom, the following DNL is obtained from the GPE :

$$i\hbar \frac{\partial \psi_j}{\partial t} = \epsilon_j \psi_j - K(\psi_{j+1} + \psi_{j-1}) + \mu_j^{loc} \psi_j. \quad (2)$$

K is the characteristic tunneling energy between adjacent sites. $\epsilon_j = \int d\vec{r} \frac{m}{2} \omega_{\parallel}^2 x^2 \Phi_j^2$ is the on-site energy resulting from the longitudinal trapping potential, which is negligible in the description of our experiment. The relevant chemical potential is given by $\mu_j^{loc} = \int d\vec{r} [\frac{m}{2} \omega_{\perp}^2 r^2 \Phi_j^2 + g_0 |\psi_j(t)|^2 \Phi_j^4]$ with $g_0 = 4\pi\hbar^2 a/m$ (a is the scattering length). It can be calculated approximately for our experimental situation assuming a parabolic shape in transverse direction (Thomas-Fermi approximation) and a Gaussian shape in longitudinal direction for $\Phi_j(\vec{r}, N_j(t))$ ($\omega_x \gg \mu_j^{loc}/\hbar > \omega_{\perp}$). This leads to $\mu_j^{loc} = U_1 |\psi_j(t)|$ with

$$U_1 = \sqrt{\frac{m\omega_{\perp}^2 g_0}{\sqrt{2\pi}\pi\sigma_x}}. \quad (3)$$

Here $\sigma_x = \lambda/(2\pi s^{\frac{1}{4}})$ is the longitudinal Gaussian width of Φ_j in harmonic approximation of the periodic potential minima. Please note, that if the local wave function Φ_j does not depend on N_j eq. 2 reduces to the well known discrete nonlinear Schrödinger equation with $\mu_j^{loc} \propto N_j$ [3, 8].

We compare the experimental and numerical results in Fig. 2 and find very good agreement. The theory reproduces the observed features such as steepening of the edges, the formation of the side peaks and the final square wave packet shape. It is important to note that all parameters entering the theory (initial width, atom number, periodic potential depth and transverse trapping frequency) have been measured independently. The observed asymmetry of the wave packet shapes (e.g. see Fig. 2, $t = 50ms$) appears due to the deviation from the perfect horizontal orientation of the wave guide ($\pm 2mrad$) which results from small changes in height of the pneumatic isolators of the optical table during the measurements.

In the following we will use the numerical results to get further insight into the self-trapping dynamics. We investigate the local tunneling dynamics and phase evolution by evaluating the relative atom number difference $\Delta N_j = (N_{j+1} - N_j)/(N_{j+1} + N_j)$ and the phase difference $\Delta\phi_j = \phi_{j+1} - \phi_j$ between two neighboring sites. In Fig. 3a) the wave packet shapes for $t = 0$ and $t = 50ms$ are shown. In Fig. 3b) we plot the relative atom number difference ΔN_j averaged over the whole propagation duration of $50ms$. The graph indicates two spatial regions

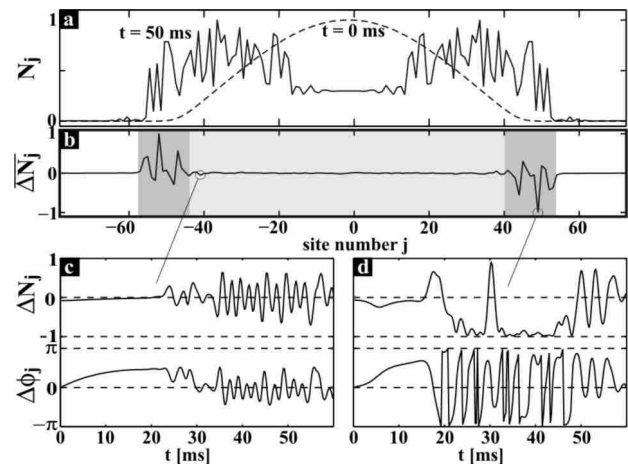


FIG. 3: A numerical investigation of the site to site tunneling dynamics. (a) The atomic distribution N_j of the wave packet for $t = 0$ and $50 ms$. (b) The relative population difference ΔN_j time averaged over the expansion time indicates two regions with different dynamics. (c) The dynamics of ΔN_j and the phase difference $\Delta\phi_j$ for the marked site oscillate around zero known as the zero-phase mode of the Boson Josephson junction. (d) The dynamics in the edge region is characterized by long time periods where $|\Delta N_j|$ is close to 1 while at the same time $\Delta\phi_j$ winds up very quickly (phase is plotted modulo π) known as 'running phase self-trapping mode' in Boson Josephson junctions. Thus the expansion of the wave packet is stopped due to the inhibited site to site tunneling at the edge of the wave packet.

with different characteristic dynamics. While the average vanishes in the central region (shaded in light gray) it has significant amplitude in the edge region (shaded in dark gray). The characteristic dynamics of ΔN_j and $\Delta\phi_j$ in the central region is depicted in Fig. 3c). The atom number difference as well as the phase difference oscillate around zero. This behavior is known in the context of BEC in double-well potentials. It is described as the Boson Josephson junction 'zero-phase mode' [2] and is characteristic for superfluid tunneling dynamics if the atom number difference stays below a critical value. At the edge in contrast, ΔN_j crosses the critical value during the initial expansion (steep density edge) and locks for long time periods to high absolute values showing that the tunneling and thus the transport is inhibited. At the same time the phase difference winds up. This characteristic dynamics has been predicted within the Boson Josephson junction model for a double-well system and is referred to as the 'running phase self-trapping mode' [2]. This analysis makes clear that the effect of nonlinear self-trapping as observed in our experiment is a *local* effect and is closely related to Boson Josephson junction dynamics in a double-well system.

Although the local dynamics just described is very complex, the evolution of the root mean square width of the wave packet, i.e. the global dynamics, can be pre-

dicted analytically within a very simple model. In [3] a Gaussian profile wave packet $\psi_j(t) \propto \exp(-(\frac{j}{\gamma(t)})^2 + i\frac{\delta(t)}{2}j^2)$ parameterized by the width $\gamma(t)$ (in lattice units) and the quadratic spatial phase $\delta(t)$, is used as an ansatz for quasimomentum $q = 0$ to solve the discrete nonlinear Schrödinger equation. The time evolution of the width $\gamma(t)$ is obtained analytically applying a variational principle. The result of this simple model is, that the dynamics of the wave packet width is solely determined by two global parameters - the density of the atoms and the depth of the periodic potential. Also a critical parameter Λ/Λ_c can be deduced, which governs the transition from the diffusive to the self-trapping regime. The transition parameter Λ/Λ_c for the 2D case described by eq. 2 is obtained following the same lines of calculation as in [3]. Assuming that the initial width $\gamma_0 \gg 1$ (in the experiment typically $\gamma_0 \approx 40$) we obtain

$$\Lambda = \frac{U_1\sqrt{N_T}}{2K} \quad \text{and} \quad \Lambda_c = \frac{3}{2} \left(\frac{9\pi}{8} \right)^{\frac{1}{4}} \sqrt{\gamma_0}.$$

A surprising result of this model is the prediction of the following scaling behavior (shown in Fig. 4):

$$\frac{\gamma_0}{\gamma_\infty} = \sqrt{1 - \frac{\Lambda_c}{\Lambda}} \quad (4)$$

for $\Lambda/\Lambda_c > 1$, where γ_∞ is the width of the wave packet for $t \rightarrow \infty$. For $\Lambda/\Lambda_c < 1$ the width is not bound and thus the system is in the diffusive regime. In the regime $\Lambda/\Lambda_c > 1$ the width is constant after an initial expansion (see inset Fig. 4). Since $\Lambda/\Lambda_c \propto \mu_{av}^{loc}/K$, the self-trapping regime is reached by either reducing the initial width, increasing the height of the periodic potential or, as is shown in Fig. 1, by increasing the number of atoms.

Scaling means that all data points (i.e. different experimental settings with the same Λ/Λ_c) collapse onto a single universal curve. In order to confirm the scaling behavior experimentally we measure the width of the wave packet after 50ms evolution for different system parameters, i.e. atom number, initial width of the wave packet, and depth of the periodic potential. The experimental results shown in Fig. 4 confirm the universal scaling dependence on Λ/Λ_c and follow qualitatively the prediction of the simple model. The dashed line in Fig. 4 is the result of the numerical integration of the discrete nonlinear equation given in eq. 2 evaluated at $t = 50ms$. It shows quantitative agreement with the experiment. The difference between the numerical (gray line) and analytical calculation (solid line) is due to the initial non-gaussian shape (numerically obtained ground state) and the strong deviation from the gaussian shape for long propagation times.

Concluding we have demonstrated for the first time the predicted effect of nonlinear self trapping of Bose-Einstein condensates in deep periodic potentials. The

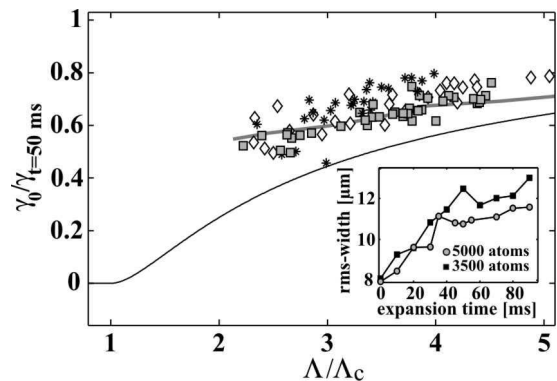


FIG. 4: Experimental investigation of the scaling behavior. The solid line shows the curve given by eq. 4. Experimentally the parameter Λ/Λ_c was varied by using three different periodic potential depths: $s = 10.6(3)$ (stars), $11.1(3)$ (squares) and $11.5(3)$ (diamonds). For each potential depth wave packets with different atom numbers and initial widths are prepared and the width for $t = 50ms$ is determined. The experimental data show qualitatively the scaling behavior predicted by eq. 4 and are in quantitative agreement with the results of the numerical integration of the DNL (gray line). The inset depicts the nature of the scaling: increasing Λ/Λ_c (by e.g. increasing the atom number) leads to a faster trapping and thus to a smaller final width.

detailed analysis shows that this is a *local* effect, which occurs due to nonlinearity induced inhibition of site to site tunneling at the edge of the wave packet. This behavior is closely connected to the phenomenon of macroscopic self trapping known in the context of double-well systems. Furthermore we quantitatively confirm in our experiments the predicted critical parameter which discriminates between diffusive and self trapping behavior.

We wish to thank A. Smerzi for very stimulating discussions. This work was supported by the Deutsche Forschungsgemeinschaft, Emmy Noether Programm, and by the European Union, RTN-Cold Quantum Gases, Contract No. HPRN-CT-2000-00125.

-
- [1] F.S. Cataliotti, S. Burger, C. Fort, P. Maddaloni, F. Minardi, A. Trombettoni, A. Smerzi, and M. Inguscio, *Science* **293**, 843 (2001).
 - [2] A. Smerzi, S. Fantoni, S. Giovanazzi, and S. R. Shenoy *Phys. Rev. Lett.* **79**, 4950 (1997); S. Raghavan, A. Smerzi, S. Fantoni, and S.R. Shenoy, *Phys.Rev. A* **59**, 620 (1999).
 - [3] A. Trombettoni and A. Smerzi, *Phys. Rev. Lett.* **86**, 2353 (2001).
 - [4] for example: D.N. Christodoulides and F. Lederer and Y. Silberberg, *Nature* **424**, 817 (2003).
 - [5] B. Eiermann, P. Treutlein, Th. Anker, M. Albiez, M. Taglieber, K.-P. Marzlin, and M.K. Oberthaler, *Phys. Rev. Lett.* **91**, 060402 (2003).
 - [6] W. Zwerger *J.Opt.B: Quantum semiclass. Opt.* **5**, S9 (2003).

- [7] A. Smerzi and A. Trombettoni, *Phys.Rev. A* **68**, 023613 (2003).
- [8] D. Hennig and G.P. Tsironis, *Phys.Rep.* **307**,333 (1999); P.G. Kevrekidis, K.O. Rasmussen, and A.R. Bishop, *Int.J.Mod.Phys.B* **15**, 2833 (2001); M. Johansson and S. Aubry, *Nonlinearity* **10**, 1151 (1997).